

Chem 4050 Project 1 Report

Charlie Li

November 7, 2025

1 Introduction

The Haber-Bosch process has been a game-changer since its invention and remains the primary industrial method for ammonia synthesis. In this process, nitrogen and hydrogen react to form ammonia under high pressure. The rate of this reaction is normally extremely slow, due to the high energy barrier to break the triple-bonded nitrogen.



The fundamental reaction of the Haber-Bosch process.

The use of an appropriate catalyst allows the Haber-Bosch process to yield a reasonable reaction rate to be of use in industry. It has been the focus of studies to optimize the reaction conditions for the Haber-Bosch process to further enhance its reaction rate and yield, which is imperative given the foundational importance of ammonia in numerous fields including agriculture and downstream industry. In this study, we explore the adsorption of nitrogen and hydrogen onto a catalyst under different conditions *in silico* to find the optimal conditions for various possible interaction schemes.

2 Methodology

Adsorption is simulated using the Grand Canonical Monte Carlo Metropolis algorithm. Simulation is performed first using a square-lattice model, and then with a hexagonal model. Different interaction schemes between adsorbed species are explored, including five neighbor-neighbor interactions and one Lennard-Jones potential model. Competitive adsorption is studied between nitrogen and hydrogen, and later ammonia is incorporated. The effect of lattice size is explored to ensure the credibility of results, and phase diagrams and animations are provided as visualization.

2.1 Grand Canonical Monte Carlo Metropolis Algorithm

We used the grand canonical ensemble to model the adsorption system. The Metropolis algorithm is used to guide the sampling from the equilibrium distribution, and 10000 steps are performed for each simulation. At each step, the addition or removal of a random particle is attempted. Later, swapping two particles and moving one particle to another empty site are also allowed. Each attempt is chosen with the same probability at each simulation step, and is accepted with the following acceptance probabilities, where N_a is the number of empty sites, N_s is the number of sites occupied by species s , ΔE is the change in total surface energy, and μ_s is the chemical potential of species s . See appendix (section 6) for derivation.

- **Addition:** $\min \left[1, \frac{N_a}{N_s+1} e^{-\beta(\Delta E - \mu_s)} \right]$
- **Removal:** $\min \left[1, \frac{N_s}{N_a+1} e^{-\beta(\Delta E + \mu_s)} \right]$
- **Swap and Move:** $\min [1, e^{-\beta \Delta E}]$

2.2 Lattice Models

A square lattice with 4×4 adsorption sites is used first. The effect of size is later examined to validate the choice. Minimum image convention is applied to model the infinite lattice surface.

A 4% Ru-Ba-K/C catalyst is an emerging catalyst for the Haber-Bosch process. Later in the study, we considered the adsorption of H_2 , N_2 and NH_3 onto ruthenium 001 surfaces, which are hexagonal. To model such a hexagonal surface, we define the unit cell as a bounding parallelogram with $\alpha = 60^\circ$. Ru bond length is calculated to be 2.645 Å from the mp-33 structure[1]. Example visualizations are shown in section 3, figure 6 and figure 7.

2.3 Interaction Schemes

In the five neighbor-neighbor interactions, the adsorbed species interacts only with its four neighbors. The adsorption energies of both H_2 and N_2 are fixed at $-0.1eV$. The interaction schemes are as follows.

- **Ideal Mixture:** The interactions between adsorbed H_2 and N_2 are ignored ($0eV$).
- **Repulsive:** The interaction energies between adsorbed H_2 and N_2 are all positive ($0.05eV$), indicating pairwise repulsion.
- **Attractive:** The interaction energies between adsorbed H_2 and N_2 are all negative ($-0.05eV$), indicating pairwise attraction.
- **Immiscible:** The interactions between the same species are negative (attractive, $-0.05eV$), while the interaction between H_2 and N_2 is positive (repulsive, $0.05eV$).
- **Like dissolve unlike:** The interactions between the same species are positive (repulsive, $0.05eV$), while the interaction between H_2 and N_2 is negative (attractive, $-0.05eV$).

To more realistically simulate the adsorption processes, adsorption energies of each species onto the Ru(001) surface are looked up from literature. Jacobi[2] found the binding energy of nitrogen gas to be $-0.5eV$, with the nitrogen binding onto the top site of Ru atoms. Ungerer and Leeuw[3] found the total adsorption energy of molecular H_2 , including its dissociation into elemental H^* , to be around $-1.34eV$. For simplicity, we assume that both H_2 and N_2 bind to the top sites, with $\epsilon_{H_2} = -1.34eV$ and $\epsilon_{N_2} = -0.5eV$, where ϵ_s is the adsorption energy of species s .

Danielson et al.[4] found that the desorption energy of NH_3 molecules from Ru(001) at low temperatures can be either $0.32eV$ or $0.46eV$ depending on its molecular states. For simplicity, we take the average and let its adsorption energy be $\epsilon_{NH_3} = -0.39eV$.

The interactions between H_2 , N_2 and NH_3 are modeled using the Lennard-Jones potential.

$$V(r) = 4\epsilon \left[\left(\frac{\sigma}{r}\right)^{12} - \left(\frac{\sigma}{r}\right)^6 \right] \quad (2)$$

12-6 Lennard-Jones Potential

The Lennard-Jones parameters are cited from the literature for same-species interactions, and calculated for different-species interactions according to the Lorentz-Berthelot mixing rules: $\sigma_{12} = \frac{\sigma_1 + \sigma_2}{2}$ and $\epsilon_{12} = \sqrt{\epsilon_1 \epsilon_2}$. The parameters used are listed in table 1.

Interaction	$\epsilon(eV)$	$\sigma(\text{\AA})$
H_2-H_2	6.6×10^{-4}	2.918
N_2-N_2	3.5×10^{-3}	3.614
H_2-N_2	1.5×10^{-3}	3.266
NH_3-NH_3	4.8×10^{-2}	2.900
H_2-NH_3	5.6×10^{-3}	2.909
3 N_2-NH_3	1.3×10^{-2}	3.257

Table 1: LJ parameters. H_2-H_2 and N_2-N_2 data from Wang et al[5]; NH_3-NH_3 data from Poling et al[6]. The rest are calculated using the Lorentz-Berthelot mixing rules.

3 Results

The following are the simulation results that allow for addition and removal attempts, using 4×4 square lattices for each of the five neighbor-neighbor interaction schemes. The phase diagrams (figure 1) are produced with various temperatures and μ_{H_2} while maintaining a constant chemical potential of $\mu_{N_2} = 0.1eV$. The lattice configurations (figure 2) are sampled from the systems at $T = 116K$ with various μ_{H_2} and interaction schemes.

The same analysis is performed with all the same conditions except for the types of allowed attempts. The simulation is enhanced by allowing for swapping two particles or moving one particle to a different empty site. The phase diagrams (figure 3) and example lattice configurations (figure 4) are produced in the same manner.

The effect of size of the square lattice is examined using different sizes varying from 1×1 to 10×10 . To observe effect of lattice size, we use the repulsive interaction scheme as an example, which makes obvious the effects of interactions, and vary the lattice sizes while keeping all the other conditions the same as above (with enhanced conditions). The results are shown in figure 5.

Further simulation is performed with 4×4 hexagonal lattices. The smallest repeating unit on this lattice is an equilateral triangle, and the bounding box is a parallelogram with $\alpha = 60^\circ$ where α is the angle between the two sides. First, competitive adsorption between H_2 and N_2 is studied on such lattices, whose interactions are modeled using the Lennard-Jones potentials. Minimum image convention is applied to model the infinite lattice surface. Realistic adsorption energies mentioned in section 2.3 are used. The effects of temperature and μ_{H_2} are explored while maintaining $\mu_{N_2} = -0.1eV$. The resulting phase diagrams and example lattices are shown in figure 6.

Next, NH_3 is incorporated in the model with the chemical potential $\mu_{NH_3} = -0.1eV$, using otherwise the exact same conditions as described above. Adsorption energies and Lennard-Jones parameters involving NH_3 are described in section 2.3. The resulting phase diagrams and example lattices are shown in figure 7.

4 Discussion

4.1 Square Matrix With Neighbor-Neighbor Interactions

We see the same trends in phase diagram 1 and phase diagram 3, demonstrating the robustness of the Metropolis algorithm. We start by discussing the trends seen from those two figures, as well as their corresponding lattices (figure 2 and figure 4).

1. Ideal Mixture

- **Temperature:** Temperature has the most observable effect when $\mu_{H_2} > -0.1eV$, where the increase of temperature leads to a decrease in θ_{H_2} but increase in θ_{N_2} . It seems that temperature

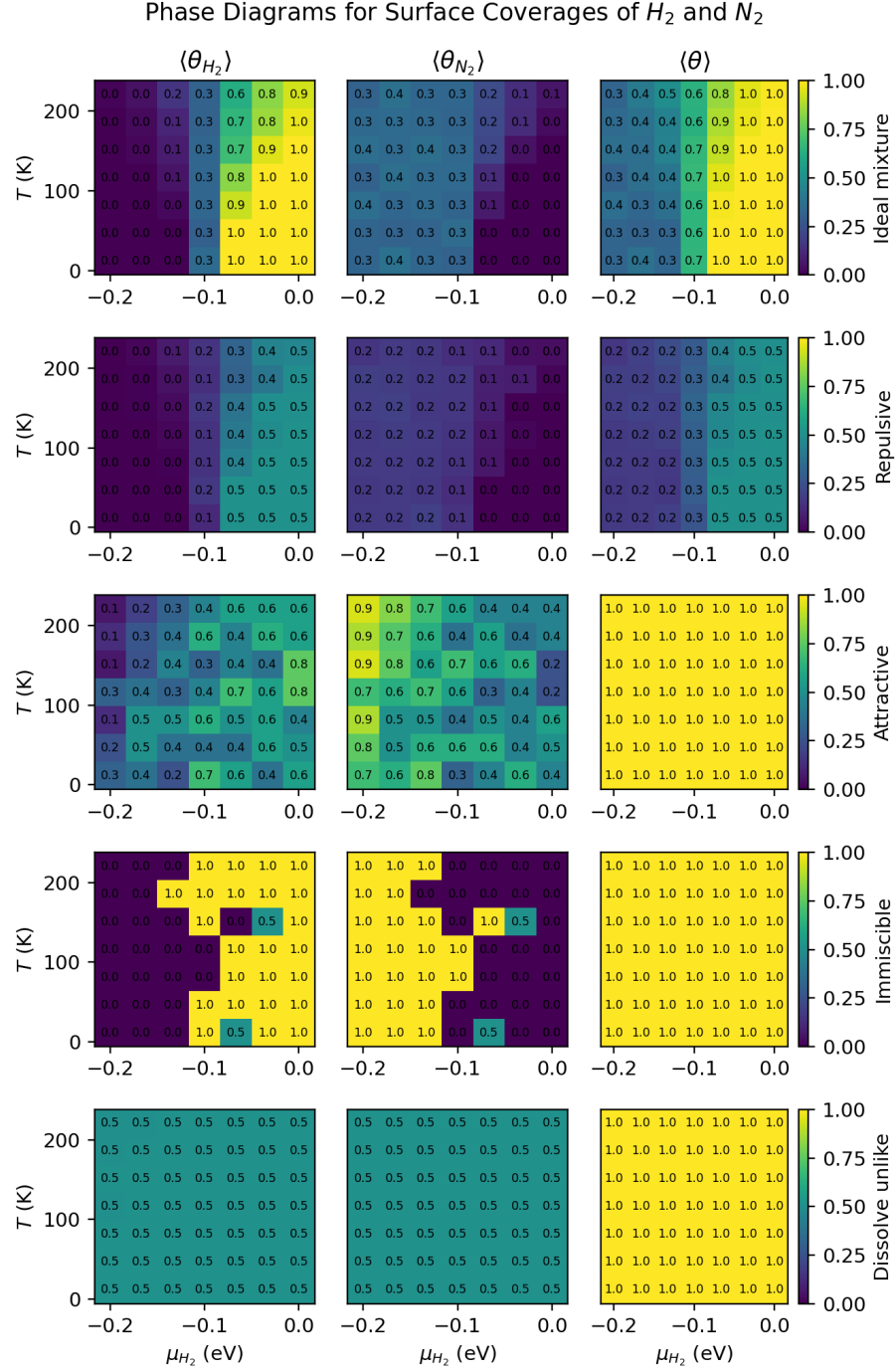


Figure 1: Phase diagrams for simulations with square lattices and neighbor-neighbor interactions. Columns show grouping by different species; rows by different interaction schemes as labeled on the color bars. X axis shows chemical potential of H_2 ; y axis shows temperature. Colors and numbers in the grids indicate mean coverage.

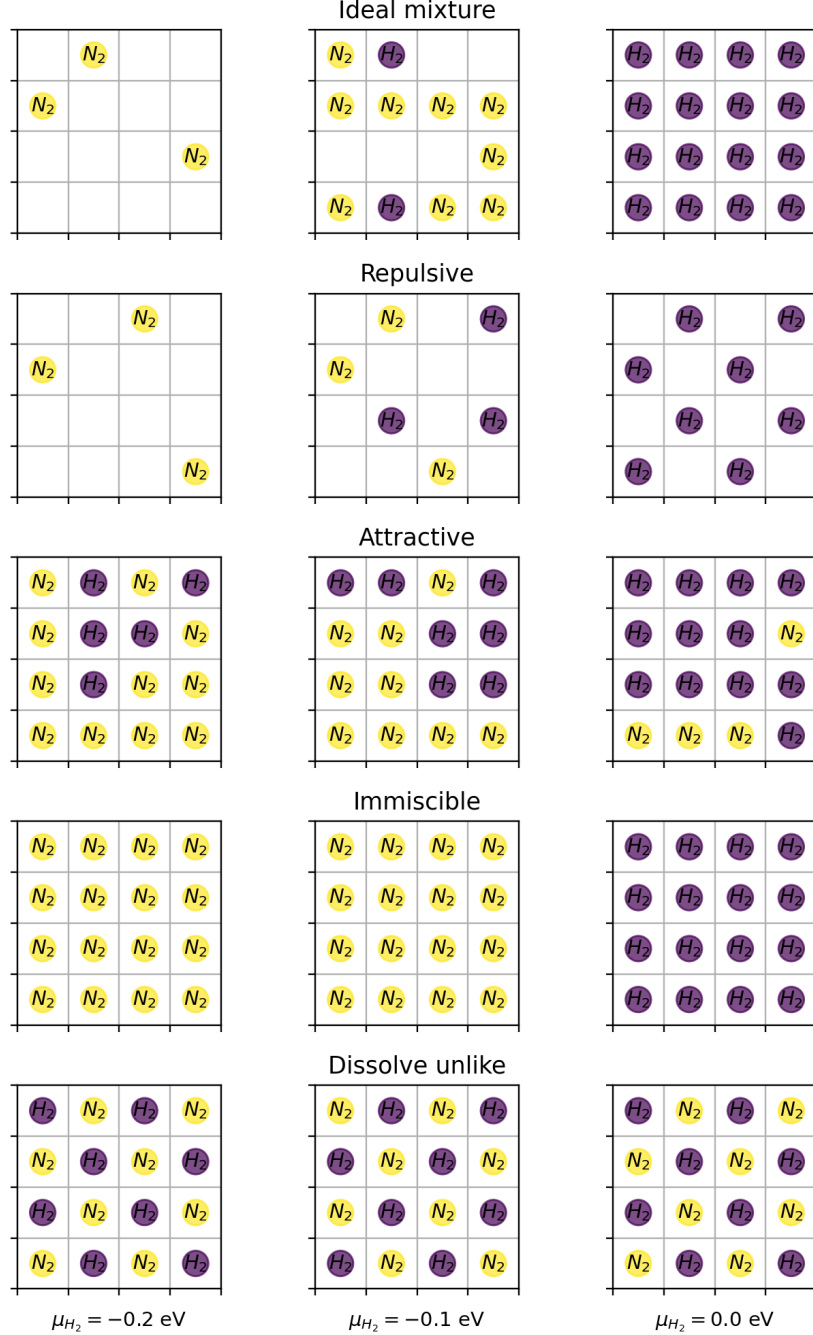
Lattice configurations at $T=116$ K for different interaction schemes

Figure 2: Example lattice configurations for simulations with square lattices and neighbor-neighbor interactions, sampled at $T = 116K$ and various μ_{H_2} . Columns show grouping by different chemical potentials of H_2 , as shown on the bottom of the figure; rows are grouped by different interaction schemes.

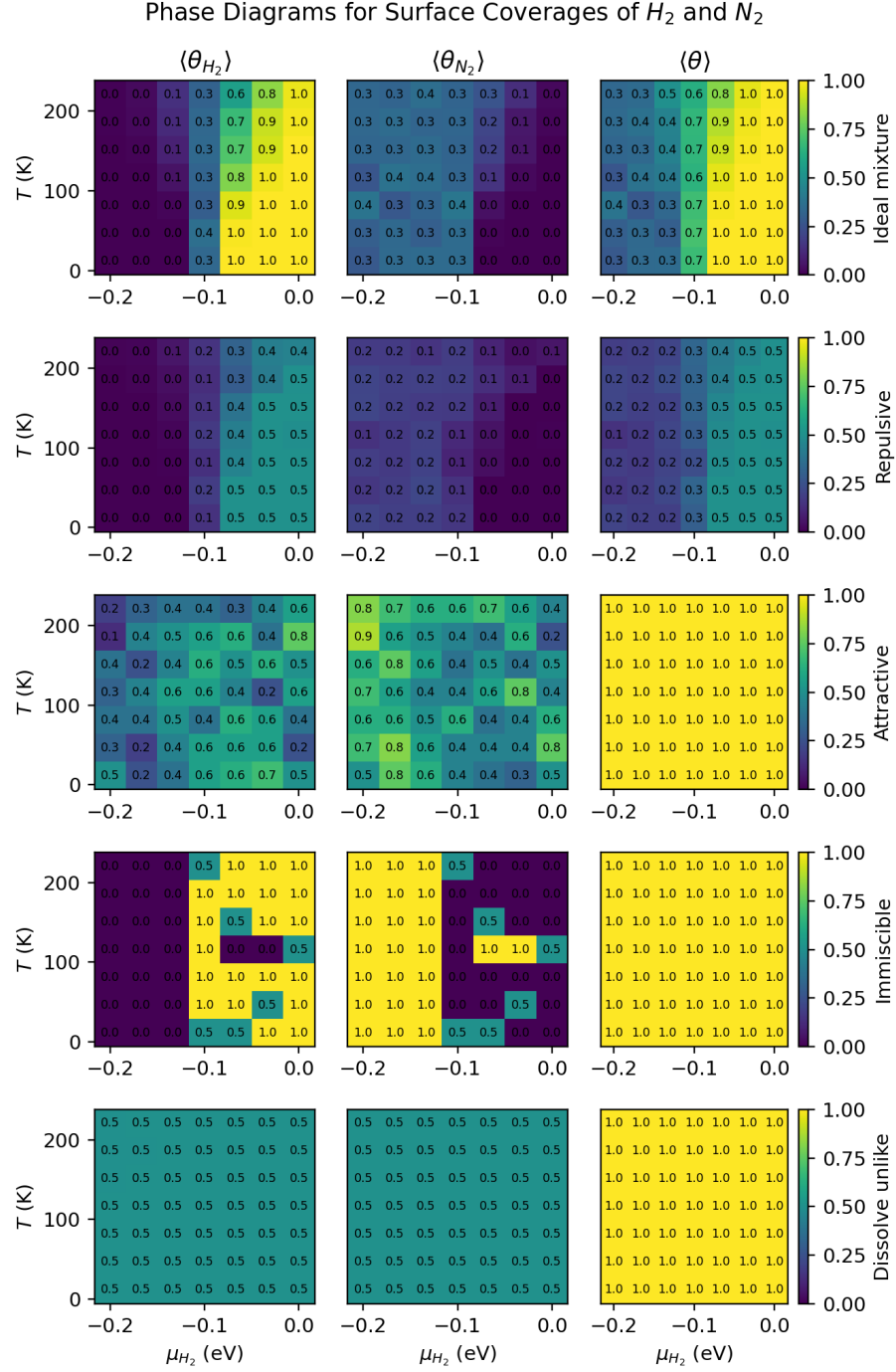


Figure 3: Phase diagrams for simulations with square lattices and neighbor-neighbor interactions with enhanced conditions (allowing for particle swapping and moving). Columns show grouping by different species; rows by different interaction schemes as labeled on the color bars. X axis shows chemical potential of H_2 ; y axis shows temperature. Colors and numbers in the grids indicate mean coverage.

Lattice configurations at T=116 K for different interaction schemes

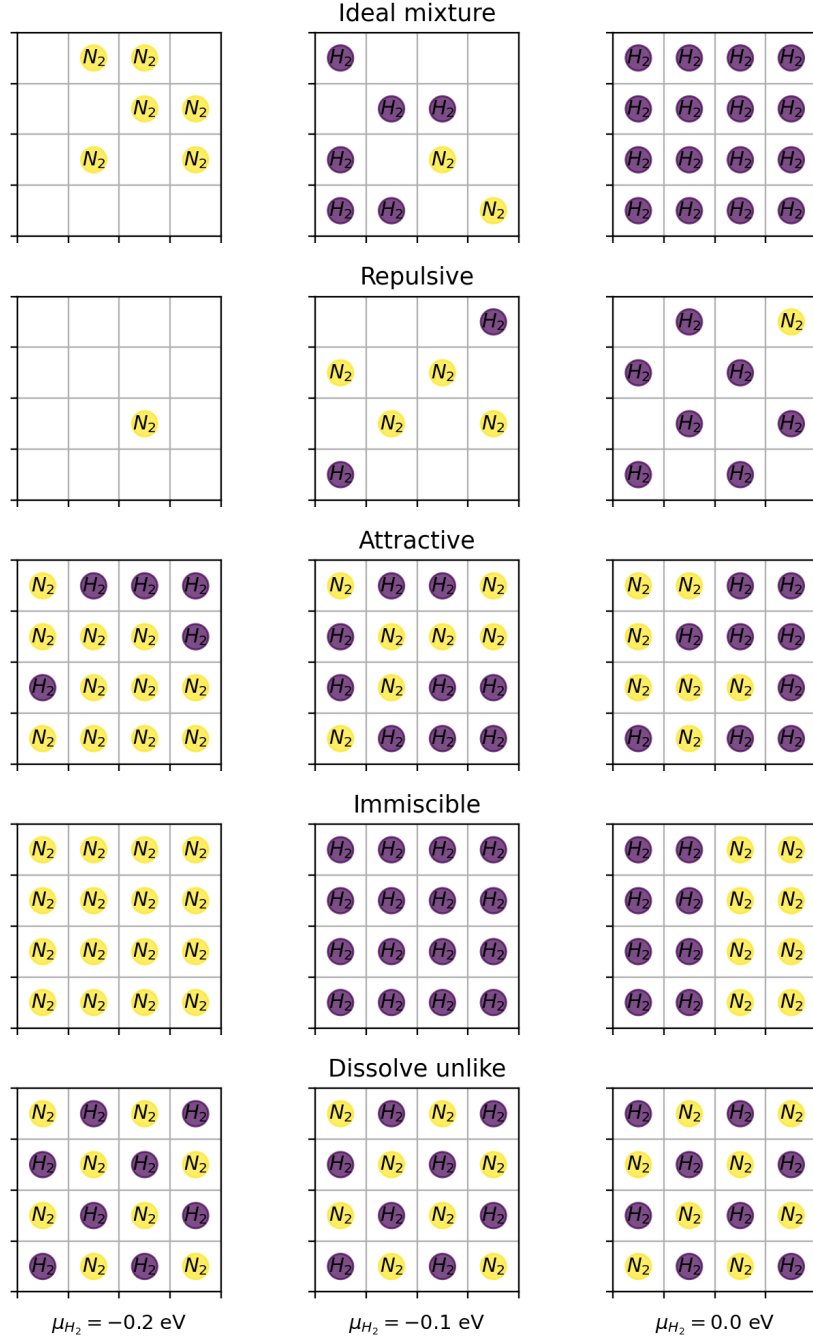


Figure 4: Example lattice configurations for simulations with square lattices and neighbor-neighbor interactions under enhanced conditions (allowing for particle swapping and moving), sampled at $T = 116K$ and various μ_{H_2} . Columns show grouping by different chemical potentials of H_2 , as shown on the bottom of the figure; rows are grouped by different interaction schemes.

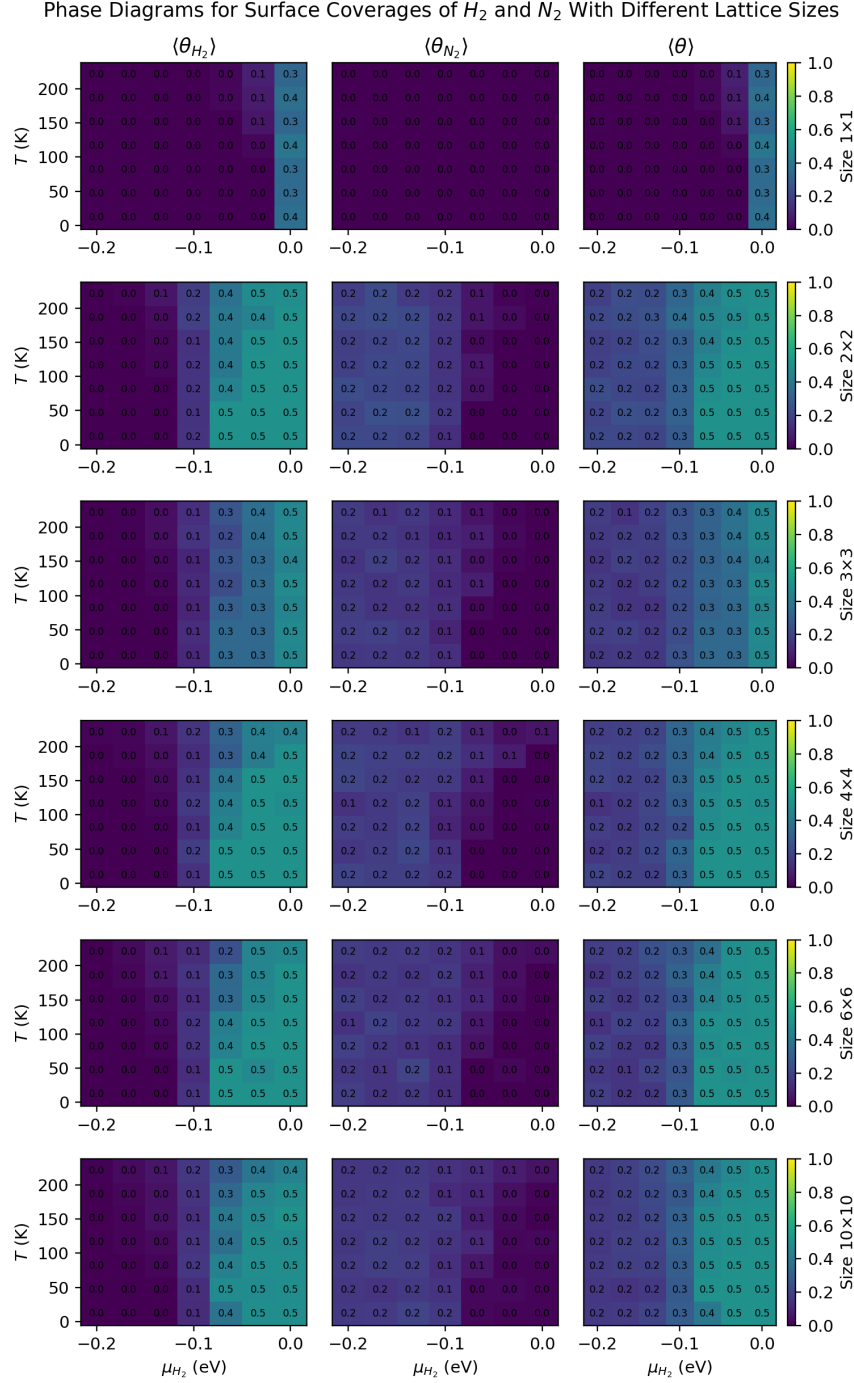


Figure 5: Phase diagrams for simulations with square lattices, neighbor-neighbor interactions and enhanced conditions using different lattice sizes. Columns show grouping by different species; rows by different lattice sizes as labeled on the color bars. X axis shows chemical potential of H_2 ; y axis shows temperature. Colors and numbers in the grids indicate mean coverage.

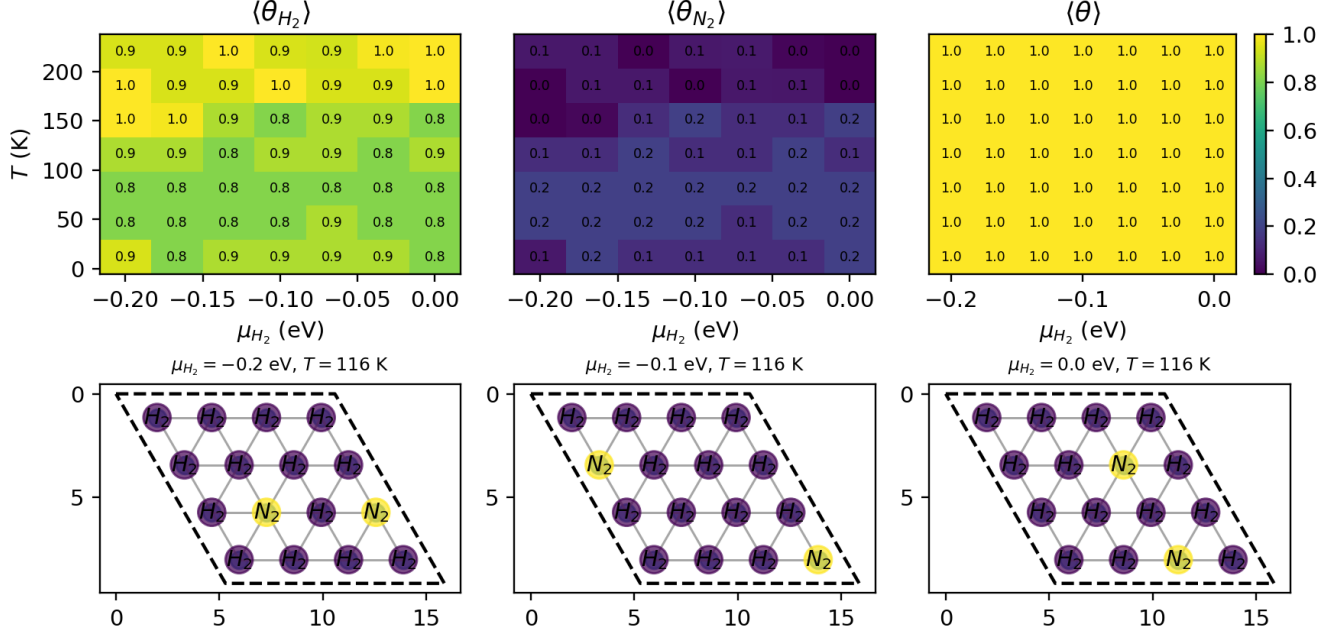
Phase Diagrams for Surface Coverages of H_2 and N_2 

Figure 6: Simulation results with hexagonal lattices and Lennard-Jones potentials. Top row: phase diagrams. Columns show grouping by different species. X axis shows chemical potential of H_2 ; y axis shows temperature. Colors and numbers in the grids indicate mean coverage. Bottom row: example lattice configurations, sampled from the systems under described temperatures and μ_{H_2} .

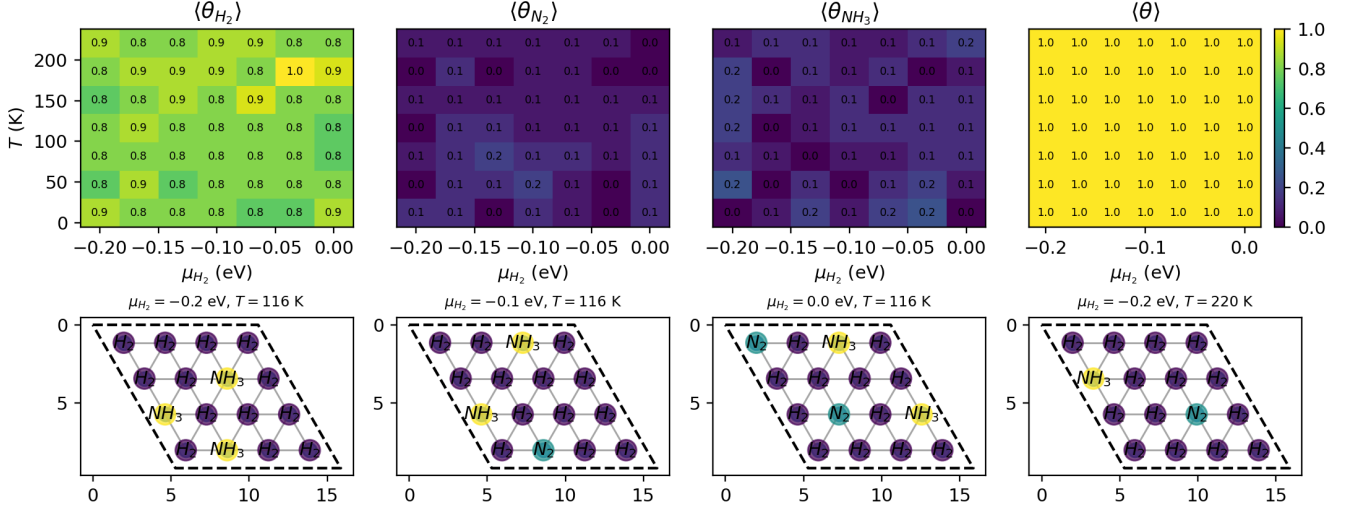
Phase Diagrams for Surface Coverages of H_2 , N_2 and NH_3 

Figure 7: Simulation results with hexagonal lattices and Lennard-Jones potentials. Top row: phase diagrams. Columns show grouping by different species. X axis shows chemical potential of H_2 ; y axis shows temperature. Colors and numbers in the grids indicate mean coverage. Bottom row: example lattice configurations, sampled from the systems under described temperatures and μ_{H_2} .

has a greater effect on the species with the greater chemical potential, as when $\mu_{H_2} < -0.1eV$, the trend is reversed. The decrease in the coverage of the species with a greater chemical potential is expected, as the gas phase has greater entropy, and an increase in temperature favors the gain in entropy by the gas phase over the gain in enthalpy by the adsorbed phase. The desorption of this species leaves space for the adsorption of the other species, leading to its increase in coverage.

- μ_{H_2} : At a given temperature, as μ_{H_2} increases, θ_{H_2} increases, while θ_{N_2} decreases. This is expected, as species seek to minimize their chemical potentials, and a higher chemical potential in the gas phase would drive H_2 into the adsorbed phase. This higher tendency to bind the surface would exclude N_2 from binding, leading to a decrease in θ_{N_2} . Since $\mu = \mu^0 + RT\ln(P/P^0)$ for an ideal gas, a higher μ means a higher pressure. It makes sense that under higher H_2 pressure, more H_2 would bind the surface, which takes the place of N_2 .
- **Optimal condition:** The optimal condition for ammonia synthesis should ideally have a ratio of 3:1 for adsorbed $H_2:N_2$, and the two species should be near each other to react. The total coverage is maximized at low temperature and high μ_{H_2} , but high μ_{H_2} also excludes N_2 from binding. The optimal condition seems to be $-0.08eV/mol < \mu_{H_2} < -0.05eV/mol$ and $125K < T < 250K$, where coverage of H_2 is around 0.7 and N_2 around 0.2. Although the total coverage is less than 1, this optimizes the ratio of $H_2:N_2$.

2. Repulsive

- **Temperature:** The same trend is observed as in the ideal mixture model, but the effect is smaller or unobservable compared with the ideal mixture.
- μ_{H_2} : With increasing μ_{H_2} , θ_{H_2} and θ increases, while θ_{N_2} decreases. This is expected with higher tendency of H_2 to leave the gas phase with higher μ . With the repulsive interaction between H_2 and N_2 , more adsorbed H_2 would lead to a greater decrease in N_2 coverage compared to the ideal mixture.
- **Compared** with the ideal mixture, θ_{H_2} , θ_{N_2} and θ all become smaller with the same T and μ_{H_2} . This is expected, as repulsion between adsorbed particles would favor the gas phase for both H_2 and N_2 . In the lattice with $\mu_{H_2} = 0$, we see that the hydrogen molecules arrange themselves alternately such that no two molecules can interact with each other. Thus, the maximum coverage achieved is 0.5. Such an interaction would make the catalyst less efficient than it would be under the ideal mixture or the attractive interaction scheme, since less coverage is achieved and fewer reaction opportunities are presented.
- **Optimal condition:** When $\mu_{H_2} > -0.05eV/mol$, the total coverage is maximized. However, almost no nitrogen is adsorbed under this condition, which would not be ideal for the synthesis of ammonia. When $-0.08eV/mol < \mu_{H_2} < -0.05eV/mol$ and $60K < T < 175K$, θ_{H_2} is around 0.4 and θ_{N_2} is around 0.1, which seems to be the best condition with a ratio of $H_2:N_2$ around 3:1. Of course, the coverages are quite low in this condition, which could be argued against it. Further experiment is needed to determine if balanced but low adsorption of both molecules is preferred over high adsorption of H_2 but low adsorption of N_2 .

3. Attractive

- **Temperature:** The effect of temperature seems to be mixed and not prominent. When $\mu_{H_2} > -0.15eV/mol$, temperature doesn't seem to have any directional impact on both θ_{H_2} and θ_{N_2} . Interestingly, when $\mu_{H_2} < -0.15eV/mol$, as temperature increases, θ_{H_2} decreases but θ_{N_2} fluctuates and even seems to increase, which is opposite the trend observed in the ideal mixture model. This might be explained by the greater statistical chance of N_2 binding and forming an attractive network with $\mu_{N_2} > \mu_{H_2}$. High temperature may not provide enough thermal energy to disrupt this network, but it has easier influence on H_2 which has a smaller chemical potential.

- μ_{H_2} : As μ_{H_2} increases, θ_{H_2} increases while θ_{N_2} decreases, which is as expected as H_2 gains larger tendency to bind.
- **Compared** with the ideal mixture, θ and θ_{N_2} become larger with the same T and μ_{H_2} , while θ_{H_2} is larger when $\mu_{H_2} < \mu_{N_2}$, but smaller when $\mu_{H_2} > \mu_{N_2}$. This is expected, as attraction between adsorbed molecules would favor the adsorbed phase. And due to the attraction between H_2 and N_2 , more N_2 can bind even when H_2 is dominant. In the lattice we see a mixture of fully occupied H_2 and N_2 due to their attraction. Such an interaction would make the catalyst more efficient, since the species bind easily and have more chances to react.
- **Optimal condition:** $\mu_{H_2} > -0.05\text{eV/mol}$ under all temperatures sampled seems to be the best condition, where θ_{H_2} is around 0.6, slightly larger than θ_{N_2} which is around 0.4, with a total coverage of 1. To save the heating cost on industrial reactors, a moderate temperature could be selected.

4. Immiscible

- **Temperature:** It seems that no effect of temperature can be concluded from the phase diagrams. This might be because the attraction between the same species is strong enough that thermal energy cannot break them, so coverage is determined solely by chemical potentials. In particular, when $\mu_{H_2} = \mu_{N_2} = -0.1\text{eV/mol}$, H_2 occupies all the sites half of the time. Since the energetics of H_2 and N_2 are perfectly symmetrical in this case, we would expect such an even distribution if temperature has no effect.
- μ_{H_2} : When $\mu_{H_2} < \mu_{N_2}$, the lattice is fully occupied by N_2 . When $\mu_{H_2} > \mu_{N_2}$, it is fully occupied by H_2 . This is as expected. Since the two species attract like and repel unlike, whichever species with the larger μ , and therefore larger tendency to bind, will win and repel the other.
- **Optimal condition:** $\mu_{H_2} = \mu_{N_2} = -0.1\text{eV/mol}$ seems to be the best condition, where each species has equal chance to dominate. However, this situation is non-ideal under all conditions, since the two species would hardly react if they repel each other. In the lattice we only observe one species under all conditions, and therefore the catalyst is likely very inefficient.

5. Like Dissolves Unlike

- Under this model, the full coverage remains 1 with H_2 and N_2 equally adsorbed in all conditions. The high coverage can be understood as the attraction network dominates over thermal fluctuation. The equal partition can be understood as the attraction network needs both species to form. In the lattice we see that H_2 and N_2 are arranged alternately such that the four neighbors of one species are the other species. This catalyst is likely very efficient, since the species bind readily and mix well with each other, presenting ample opportunities to react with each other.
- **Optimal condition:** There is no difference between all the conditions sampled. Considering the cost of heating and high pressure, the optimal condition should be with low temperature and low μ_{H_2} . However, low temperature would also lead to slow reaction rates. Therefore, a tradeoff between heating cost and reaction rate must be made.

4.2 Effect of Square Lattice Size

Since minimum image convention is used, the size of the square lattice is expected to have no influence on adsorption behavior provided that it is more than twice the interaction cutoff. For the square lattice with neighbor-neighbor interactions (cutoff = 1), this means that the lattice should ideally be at least 3×3 .

Regardless of the cutoff, lattice size would have no impact on the ideal mixture at all, since no interaction is modeled. To observe effects of lattice size, we used the repulsive interaction scheme as an example, since

the interactions have obvious effects in that model. Simulations were run on square lattices with repulsive interactions with different size $n \times n$, with the results shown in figure 5.

As expected, when $n < 2$, the resulting phase diagram deviates from the others. When $n > 2$, the resulting phase diagrams are consistent with each other. When $n = 2$, the results also look reasonable but represent an edge case that should not be trusted.

4.3 Realistic Conditions

Two simulations were performed using the realistic conditions described in section 2.3. In these simulations, 4×4 hexagonal lattices were used with the Lennard-Jones potentials modeling the interactions. The choice of a 4×4 lattice could be justified by examining the Lennard-Jones curves shown in figure 8. Note that our system is discrete with allowed distances l , $\sqrt{3}l$, $2l$, etc, where $l = 2.645\text{\AA}$. The interactions are basically 0 when the particles are $22.645 = 5.29\text{\AA}$ away, which indicates the appropriateness of using the minimum image convention on 4×4 lattices.

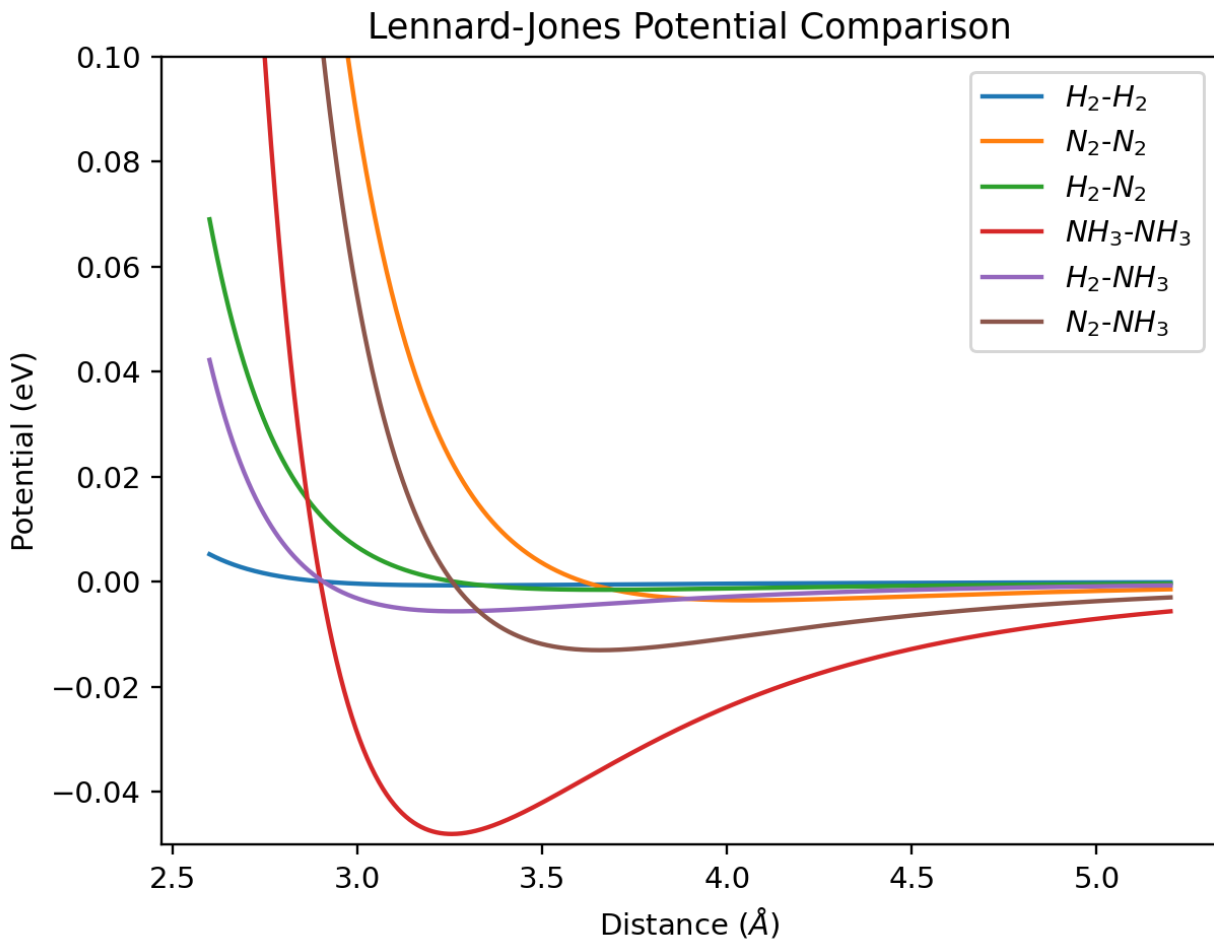


Figure 8: Lennard-Jones potential curves, using the parameters described in section 2.3. Note that our system is discrete with allowed distances l , $\sqrt{3}l$, $2l$, etc, where $l = 2.645\text{\AA}$.

The first simulation explored the competitive adsorption between H_2 and N_2 , with the resulting phase diagrams and lattice configurations shown in figure 6. From figure 8, we observe that the attractions are much weaker than repulsions. H_2 weakly repels with itself, while all the other pairs repel strongly when 1-bond (2.645\AA) apart. Combined with the large adsorption energy of -1.34eV for H_2 , it makes sense that H_2 always dominates on the surface, which is not affected by changes in μ_{H_2} . The attractive network of H_2 is strong, and the incorporation of N_2 could be unfavorable due to repulsion. Increasing temperature favors the adsorption of H_2 , which could be understood as the thermal energy exceeds the adsorption energy of N_2 but not that of H_2 , which leads to favorable adsorption of H_2 . $T < 150K$ seems to be the optimal condition in this model, which results in μ_{H_2} around 0.8 and μ_{N_2} around 0.2.

The second simulation explored the competitive adsorption between H_2 , N_2 and NH_3 , with the resulting phase diagrams and lattice configurations shown in figure 7. This is closer to the actual industrial condition, where NH_3 might not be immediately separated from the reaction mixture. The same interpretations can be made for this model as the previous 2-species competitive model. Although NH_3 has a large ϵ and therefore a stronger maximal attraction, our lattice is a discrete system with the two nearest distances being 1-bond (2.645\AA) and $\sqrt{3}$ -bond (4.581\AA) long, where the repulsion of NH_3-NH_3 is very strong (at 2.645\AA) but the attraction quite weak (at 4.581\AA). Since the adsorption energy of NH_3 is also quite small, it is expected to behave similarly to N_2 . H_2 is still expected to dominate due to its weak repulsion and large adsorption energy.

4.4 Animations

Animations showing the stochastic nature of the simulation systems can be found in the *animations* folder.

5 Conclusion

In this study, we explored the adsorption behaviors of the relevant species in the Haber-Bosch process. We started by exploring the competitive adsorption of H_2 and N_2 onto a square lattice under different possible neighbor-neighbor interaction schemes, and later introduced more realistic models including hexagonal lattices and Lennard-Jones interactions, as well as involving NH_3 in the competition. From equation 1, it is expected that the rate of reaction should be highest when $\langle\theta_{H_2}\rangle : \langle\theta_{N_2}\rangle = 3 : 1$ and if the two species are close to each other. We identified the optimal conditions for each of the interaction schemes and noted the potential problems posed by some of the interaction schemes. Such insights could be applied to the design of industrial reactors with optimal temperature and pressure in mind, once better understanding of the interactions between the involved species is achieved. The insights and methods in this study could also be applied to other systems with similar interaction schemes.

When running the simulation with realistic parameters, it is noted that although the total coverage remains high, nitrogen usually has a low coverage. To further optimize the Haber-Bosch process under these conditions, the following could be considered:

1. Increase the pressure, and therefore the chemical potential, of N_2 , which has a smaller adsorption energy compared to H_2 and stronger repulsion. This is the most straightforward way to help more N_2 bind to the surface. However, the pressure durability of the reactor and the costs associated with it also need to be taken into consideration.
2. Remove ammonia, therefore lowering its chemical potential. This would further lower the coverage of NH_3 on the surface, preventing it from blocking reaction sites.

3. Temperature does not have a great influence on the coverages, but it does on reaction rates. A moderate temperature should be applied to enable faster reactions once the species bind on the surface, but applying a high temperature could increase costs.
4. Given that hydrogen binds strongly on the surface, its pressure could be lowered to allow for more binding of nitrogen. Nitrogen is also significantly cheaper than hydrogen since it can be directly separated from air, making it more cost-effective to flood the system with nitrogen.

However, certain caveats of the current model should also be noted, which could be improved by future studies.

1. N_2 and H_2 interact through induced dipoles, which can be reasonably modeled by the Lennard-Jones potential. However, ammonia has a strong dipole moment and can hydrogen bond, which makes the Lennard-Jones model inaccurate. To model the binding of ammonia more accurately, a force field should be selected that takes into account these additional, directional interactions.
2. It is possible that different molecules have different preferences for binding sites. For example, hydrogen might preferentially bind at the fourfold sites. A more accurate model could allow for three kinds of binding sites to have different adsorption energies and different interaction distances.
3. More sophisticated lattice models could be implemented that consider non-homogeneous sites in real-world catalysts, which are usually a blend of different materials.

6 Appendix: Derivation of the Acceptance Probabilities

We derive the acceptance probabilities for addition, removal, swapping and moving particles using detailed balance, which states that

$$\alpha(\vec{r} \rightarrow \vec{r}') \times acc(\vec{r} \rightarrow \vec{r}') \times p(\vec{r}) = \alpha(\vec{r}' \rightarrow \vec{r}) \times acc(\vec{r}' \rightarrow \vec{r}) \times p(\vec{r}') \quad (3)$$

where \vec{r} is the current state, \vec{r}' is the new state, α is the proposal probability for the state change, acc is the acceptance probability for the state change, and p is the probability distribution of the corresponding state. For a grand canonical system, the probability distribution is given in equation 4, where N_i is the number of particles for the i^{th} species, $E(\mathbf{N})$ is the total surface energy, μ_i is the chemical potential of species i , and Z is the partition function, which is constant for a given system.

$$p(\mathbf{N}) = \frac{e^{-\beta[E(\mathbf{N}) - \sum \mu_i N_i]}}{Z} \quad (4)$$

6.1 Addition

For adding a particle of species s , the proposal probability of adding to one of the N_a empty sites is $\alpha(\vec{r} \rightarrow \vec{r}') = \frac{1}{N_a}$, while the proposal probability of the reverse process (removing one of species s from $N_s + 1$ sites, where N_s is the number of occupied sites of species s at the current timestep) is $\alpha(\vec{r}' \rightarrow \vec{r}) = \frac{1}{N_s + 1}$. Therefore,

$$\frac{acc(\vec{r} \rightarrow \vec{r}')}{acc(\vec{r}' \rightarrow \vec{r})} = \frac{\alpha(\vec{r}' \rightarrow \vec{r})p(\vec{r}')}{\alpha(\vec{r} \rightarrow \vec{r}')p(\vec{r})} = \frac{N_a}{N_s + 1} \cdot \frac{\exp[-\beta(E(\mathbf{N}') - (\sum \mu_i N_i + \mu_s))]}{\exp[-\beta(E(\mathbf{N}) - (\sum \mu_i N_i))]} = \frac{N_a}{N_s + 1} e^{[-\beta(\Delta E - \mu_s)]} \quad (5)$$

Therefore, we have

$$acc(\vec{r} \rightarrow \vec{r}') = \min \left[1, \frac{N_a}{N_s + 1} e^{[-\beta(\Delta E - \mu_s)]} \right] \quad (6)$$

6.2 Removal

Similar to addition, for removing a particle of species s , the proposal probability of choosing from N_s occupied sites is $\alpha(\vec{r} \rightarrow \vec{r}') = \frac{1}{N_s}$, while the proposal probability of the reverse process (adding one of species s to $N_a + 1$ sites, where N_a is the number of empty sites at the current timestep) is $\alpha(\vec{r}' \rightarrow \vec{r}) = \frac{1}{N_{a+1}}$. Therefore,

$$\frac{\text{acc}(\vec{r} \rightarrow \vec{r}')}{\text{acc}(\vec{r}' \rightarrow \vec{r})} = \frac{\alpha(\vec{r}' \rightarrow \vec{r})p(\vec{r}')}{\alpha(\vec{r} \rightarrow \vec{r}')p(\vec{r})} = \frac{N_s}{N_a + 1} \cdot \frac{\exp[-\beta(E(\mathbf{N}') - (\sum \mu_i N_i - \mu_s))]}{\exp[-\beta(E(\mathbf{N}) - (\sum \mu_i N_i))]} = \frac{N_s}{N_a + 1} e^{[-\beta(\Delta E + \mu_s)]} \quad (7)$$

6.3 Swapping and Moving

For swapping two particles (allowing sampling the same particle twice), $\alpha(\vec{r} \rightarrow \vec{r}') = \alpha(\vec{r}' \rightarrow \vec{r}) = 1/N_o^2$ where N_o is the number of all occupied sites. For moving one particle to an empty site, $\alpha(\vec{r} \rightarrow \vec{r}') = \alpha(\vec{r}' \rightarrow \vec{r}) = 1/(N_o \times N_a)$, where N_a is the number of empty sites. Therefore, we have symmetrical proposal probabilities, and since chemical potentials don't change, the acceptance probabilities are

$$\text{acc}(\vec{r} \rightarrow \vec{r}') = \min \left[1, \frac{p(\vec{r}')}{p(\vec{r})} \right] = \min \left[1, e^{-\beta[(E' - \sum \mu'_s N'_s) - (E - \sum \mu_s N_s)]} \right] = \min \left[1, e^{-\beta \Delta E} \right] \quad (8)$$

for both scenarios.

References

- [1] Materials Project. Materials Project. <https://next-gen.materialsproject.org/materials/mp-33?formula=Ru> (accessed 2025-11-06).
- [2] Jacobi, K. Nitrogen on Ruthenium Single-Crystal Surfaces. *Phys. Status Solidi A* **2000**, *177* (1), 37–51. [https://doi.org/10.1002/\(sici\)1521-396x\(200001\)177:1%3C37::aid-pssa37%3E3.0.co;2-y](https://doi.org/10.1002/(sici)1521-396x(200001)177:1%3C37::aid-pssa37%3E3.0.co;2-y).
- [3] Ungerer, M. J.; Leeuw, N. H. de. Thermodynamics of Hydrogen Adsorption on Ruthenium *Fcc* Surfaces: A Density Functional Theory Study. *Phys. Chem. Chem. Phys.* **2025**, *27* (11), 5759–5772. <https://doi.org/10.1039/d4cp04165h>
- [4] Danielson, L. R.; Dresser, M. J.; Donaldson, E. E.; Dickinson, J. T. Adsorption and Desorption of Ammonia, Hydrogen, and Nitrogen on Ruthenium (0001). *Surf. Sci.* **2002**, *71* (3), 599–614. [https://doi.org/10.1016/0039-6028\(78\)90450-8](https://doi.org/10.1016/0039-6028(78)90450-8).
- [5] Wang, S.; Hou, K.; Heinz, H. Accurate and Compatible Force Fields for Molecular Oxygen, Nitrogen, and Hydrogen to Simulate Gases, Electrolytes, and Heterogeneous Interfaces. *J. Chem. Theory Comput.* **2021**, *17* (8), 5198–5213. <https://doi.org/10.1021/acs.jctc.0c01132>.
- [6] Poling, B. E.; Praunitz, J. M.; O'connell, J. P. *The Properties of Gases and Liquids*; McGraw-Hill, 2000.